JOC The Journal of Organic Chemistry

Article

pubs.acs.org/joc

Synthesis and Analysis of the All-(*S*) Side Chain of Phosphomycoketides: A Test of NMR Predictions for Saturated Oligoisoprenoid Stereoisomers

Jeffrey Buter,[†] Edmund A.-H. Yeh,[‡] Owen W. Budavich,[‡] Krishnan Damodaran,[‡] Adriaan J. Minnaard,*[,†] and Dennis P. Curran*[,‡]

[†]Stratingh Institute for Chemistry, University of Groningen, Nijenborgh 7, 9747 AG Groningen, The Netherlands

[‡]Department of Chemistry, University of Pittsburgh, Pittsburgh, Pennsylvania 15260, United States

Supporting Information

ABSTRACT: (4*S*,8*S*,12*S*,16*S*,20*S*)-Pentamethylheptacosan-1-ol has been synthesized and analyzed by resolution-enhanced NMR spectroscopy with the aid of a recent set predicted spectra of all its stereoisomers. The configuration was confirmed, but isomer purity of the sample (~70%) was lower than expected. A truncated analogue, (2*S*,6*S*,10*S*,14*S*)-2,6,10,14-tetramethylhenicosan-1-ol TBDPS ether, was prepared from a late stage synthetic intermediate. Analysis of its spectra confirmed the configuration and showed that the sample was isomerically pure. The results suggest that a late-stage epimerization, not a failure of an asymmetric synthesis step, caused the formation of minor stereoisomers in the sample of pentamethylheptacosan-1-ol. The study shows the value of the predicted set of oligoisoprenoid spectra and further extends the predictive model to a new subclass of compounds.

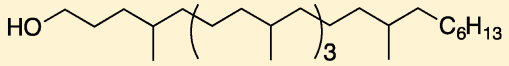

predicted ^{1}H and ^{13}C NMR spectra are used to assess structure and purity of MPM side chain samples

INTRODUCTION

β-Mannosyl phosphomycoketides (MPMs) **1** and **2** (Figure 1a) are potent T-cell antigens produced by *Mycobacterium avium* and *Mycobacterium tuberculosis*.[1] They are composed of β-D-mannose and a long, aliphatic chain linked together as a phosphate diester. In MPM biosynthesis, the polyketide side chain is formed from a fatty acid precursor by repetitive incorporation of malonyl and methyl malonyl CoA followed by full reduction.

Although MPM's side chains have a polyketide origin, a large part of the chain **3c** (C2−C21) bears methyl groups on every fourth carbon and therefore resembles a saturated oligoisoprene. In polymer terminology, such repeat units are also called alternating propylene/ethylene co-oligomers or 1-methyltetramethylene oligomers.[2] Rigorously assigning the configurations of the five side chain stereocenters of such oligomers is difficult.

Crich intentionally synthesized a mixture of MPMs **1** (R = *n*-C_4H_9) with complete stereocontrol of the mannosyl anomeric center but with all possible configurations of the side-chain stereocenters.[3] Analysis of this mixture of 32 stereoisomers confirmed the constitution of **1**. Minnaard later synthesized a pentamethylheptacosan-1-ol side chain with all five side-chain stereocenters in the (*S*)-configuration (all-(*S*)-**3c**, Figure 1b) and coupled this to β-mannose phosphate to make MPM **2** (R = *n*-C_6H_{13}).[4] This sample was assayed against Crich's mixture and a natural product sample and exhibited activity similar to that of the natural product.[5]

The five stereocenters of the side chains of **1** and **2** are biosynthesized in an iterative way by the polyketide synthase Pks12 and therefore presumably have the same configuration.[1,6] This means that the 1,4-relative configurations of the methyl-

(a) β-D-mannosyl phosphomycoketide (MPM) natural products

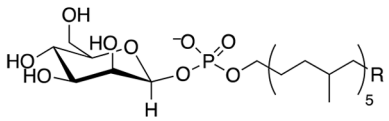

1, R = *n*-C_4H_9, **2**, *n*-C_6H_{13}

(b) Possible side chain stereostructure for ***2***

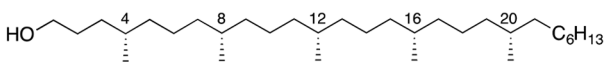

"all-(*S*)"-**3c** –or– "all-*syn*"-**3c**
(4*S*,8*S*,12*S*,16*S*,20*S*)-4,8,12,16,20-pentamethylheptacosan-1-ol

(c) Homologous series of saturated polyisoprenoids

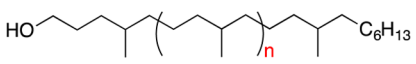

n = 1, **3a**; 4,8,12-trimethylnonadecan-1-ol
n = 2, **3b**; 4,8,12,16-tetramethyltricosan-1-ol
n = 3, **3c**; 4,8,12,16,20-pentamethylheptacosan-1-ol

Figure 1. Structures of MPM natural products and side chains.

Received: March 13, 2013
Published: April 12, 2013

Scheme 1. Synthesis of Two Samples for NMR Analysis[a]

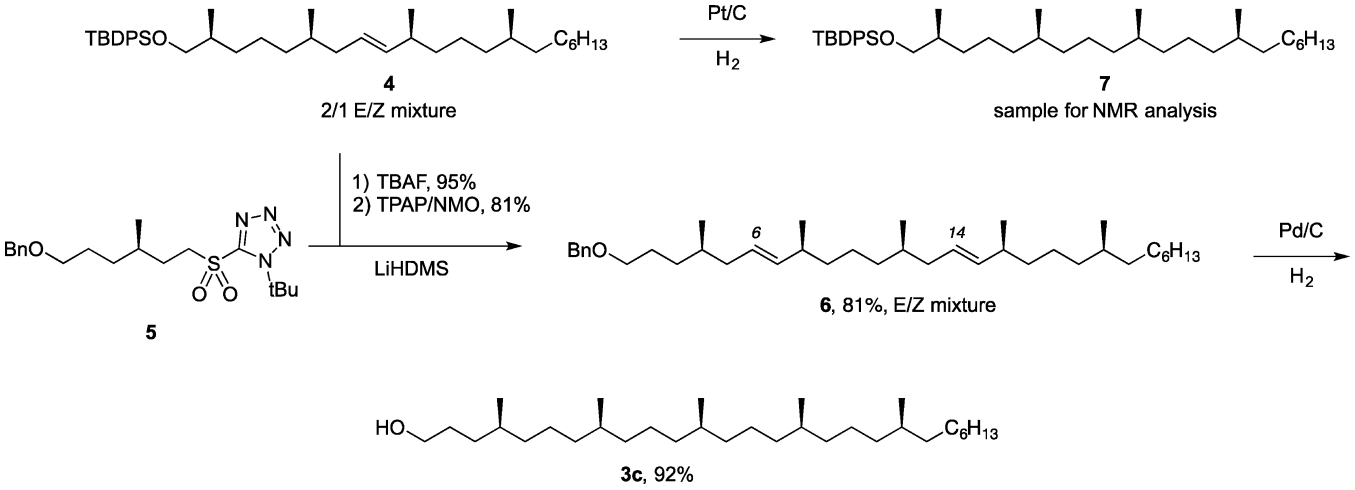

[a]**3c** is the complete MPM side chain, and **7** is a saturated derivative of key late-stage intermediate **4**.

branched stereocenters are *syn*. Of the two remaining configurations, all stereocenters (*R*) or all (*S*), the results of the bioassays support the all-(*S*) assignment of **2**.[4a,5] In addition, the crystal structure of CD1c bound to all-(*S*)-MPM **2** has been reported recently.[7] However, assignment of the absolute configuration as all-(*S*) contradicts a predictive model by Leadley and co-workers.[8] Therefore, spectroscopic or chemical means to assess the side-chain configurations is needed both to confirm the structure of the natural product and to assay structures and purities of synthetic samples.[9]

Recently we synthesized all four diastereomers of the truncated MPM side-chain model 4,8,12-trimethylnonadecanol **3a** (Figure 1c).[10] The methyl regions of both the ^{1}H and ^{13}C NMR spectra of the four isomers exhibited small but reliable differences depending on whether the nearest neighbor methyl groups were *syn* or *anti*. We used the data to predict the ^{1}H and ^{13}C NMR spectra of all stereoisomers of higher saturated oligoisoprenoids including **3b** (8 isomers) and **3c** (16 isomers). Unfortunately, it is not possible to test these predictions retrospectively with published spectra because special conditions for processing are required to enhance resolution.

Here we report the synthesis of a new sample of all-(*S*)-**3c**. Analyses of resolution-enhanced NMR spectra prove that the sample is predominately all-(*S*) but also show that the isomer ratio is lower than expected. Further analysis of a lower homologue prepared from synthetic intermediates suggests that the impurities arose not because an asymmetric synthesis step was compromised, but instead because of a late-stage partial epimerization. Just as the predicted spectra help to analyze the experimental spectra, the reverse is also true. The new chemical shift values obtained from the experimental spectra help to refine and expand the NMR model.

RESULTS AND DISCUSSION

Synthesis of the Samples. The synthesis of the new sample of **3c** was based on the catalytic enantioselective synthesis of β-D-mannosyl phosphomycoketide reported by Minnaard and co-workers.[4a,11] The late stages of this synthesis are summarized in Scheme 1, while the Supporting Information provides complete information on reagents and yields in Schemes S1 and S2. All five of the stereocenters in penultimate intermediates **4** and **5** were synthesized by asymmetric conjugate additions reactions in with high levels of stereoselectivity (>95%).

The two compounds analyzed in detail were late-stage derivative **7**, which is a phytanyl-type oligoisoprenoid with a silyl-protected hydroxy group on the left end and four repeating stereocenters, and **3c**, which is the full MPM side chain with five repeating stereocenters. Both samples were derived from unsaturated silyl ether **4**, itself made as a 2/1 mixture of *E*/*Z* isomers in a Kocienski–Julia reaction.[12]

The silyl ether **4** was desilylated (95%), and the resulting alcohol was oxidized to an aldehyde (81%). This in turn was added to the anion derived from sulfonyl tetrazole **5** to give **6** as an *E*/*Z* mixture at both the existing (C14) and the newly formed (C6) alkene (81%). Hydrogenation of the alkenes in **6** occurred simultaneously with reductive debenzylation to provide the MPM side chain sample **3c**.

Subsequent NMR studies of the final product **3c** (see below) led us to question the stereochemical integrity of **4**. To assess this, we saturated a small sample of the *E*/*Z* isomer mixture of **4** to give **7**. This sample was isomerically pure (see below) so by implication all the reactions leading to **4** (see Scheme S1 in the Supporting Information) occurred with high stereoselectivity, and the so-formed stereocenters were retained with fidelity.

Analysis of the Spectra of 3c. To assess the structure and isomeric purity of **3c**, the observed resonances in the methyl regions of both its ^{1}H and ^{13}C NMR spectra were compared with recent predictions.[10] The basis for predicting the resonances of any isomer of **3c** (n = 3) from the observed resonances of **3a** (n = 1) is shown in Figure 2. Briefly, we divide the spectrum into three parts, the left-end, the middle, and the right-end, and then add in resonances of the branched methyl groups from the model set (all isomers of **3a**) that have the appropriate stereochemical relationship to match those in **3c**. End Me groups can be *syn* or *anti*, while middle ones can be *syn*/*syn*, *anti*/*anti*, or *anti*/*syn* (or *syn*/*anti*).

To predict a spectrum of the all-*syn* isomer of **3c** (all-(*S*)-**3c** or all-(*R*)-**3c**), we simply take the spectrum of all-*syn* **3a** and multiply the middle resonances by three (because all three middle Me groups have *syn*/*syn* relationships), as shown in Figure 2a. Figure 2b lists the remaining resonances from the complete model set. These are not used for all-*syn*-**3c** but are needed to predict spectra of its stereoisomers.

dx.doi.org/10.1021/jo4005298 | J. Org. Chem. 2013, 78, 4913–4918

*(a) Predicted NMR spectra of all-syn **3c***
multiply by 3x the middle resonance of all-*syn*-**3a**

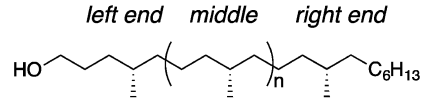

^{13}C NMR, all-*syn*-**3a**	19.67	19.79	19.77
^{1}H NMR, all-*syn*-**3a**	0.874	0.844	0.840

all-*syn*-**3a**, n = 1
all-*syn*-**3c**, n = 3

(b) Unused model peaks
present in other isomers of **3a**

Me	stereochem	^{13}C	^{1}H
left	*anti*	19.61	0.872
middle	*syn/anti*[a]	19.73	0.842
middle	*anti/anti*	19.66	0.841
right	*anti*	19.70	0.839

a) or *anti/syn*

Figure 2. Basis for predictions of NMR spectra of all-*syn*-**3c** and stereoisomers.

Standard spectra of all-*syn*-**3c** were first recorded in the usual way at 400 MHz. These compared favorably to the spectra of the prior sample[4a] but as expected did not provide information about isomer identity or purity. A new set of spectra were then recorded at 700 MHz for ^{1}H and 175 MHz for ^{13}C, and the data sets were processed by the Traficante algorithm[13] for resolution enhancement.

Figure 3a,b shows the methyl regions of the ^{13}C and ^{1}H NMR spectra, both predicted (bottom spectrum) and actual (top spectrum). The processing renders the spectra of such samples interpretable for the first time.

The predicted ^{13}C NMR spectrum of all-*syn*-**3c** (Figure 3a, bottom) shows three peaks: the left-end Me resonates at 19.67 ppm, while the right-end Me resonates at 19.77 ppm. The predicted chemical shift of the three middle methyl groups (on C8, C12, C16) is 19.79 ppm, with a relative intensity of three.

The experimentally obtained ^{13}C NMR spectrum (Figure 3a, top) is at first glance much more complex. There are 10 resonances grouped in two sets of five with a ratio of about 70/30. Thus, the sample is not isomerically pure. Three of the five peaks of the major set (19.79, 19.77, and 19.67 ppm) match perfectly (<10 ppb difference) to the predicted peaks. The two most downfield major peaks at 19.80 and 19.81 ppm are slightly downfield from their predicted location at 19.79 ppm.

We compared the major set of resonances in the experimental spectrum of all-*syn*-**3c** to the predicted spectra of all 16 isomers of **3c**,[10] and none matches as well as the spectrum of the all-*syn*-isomer. Thus, we conclude that the five major peaks in the actual spectrum in Figure 3a belong to all-*syn*-**3c**. This means that the predicted spectrum in Figure 3a is only partially correct. Because the model **3a** is too simple (it has only one middle unit), it cannot anticipate the very small differences in chemical shifts of the three "repeating" methyl groups in the middle of all-*syn*-**3c**. Indeed, given their chemical and stereochemical similarity, it is remarkable that separate resonances for these methyl groups are observed.

The methyl regions of the predicted and experimental ^{1}H NMR spectra of all-*syn*-**3c** are shown in Figure 3b. The predicted spectrum is again simpler than the actual one. Now there is an additional resonance; the triplet at 0.882 ppm is the

(a) actual (top) and predicted (bottom) ^{13}C NMR spectra

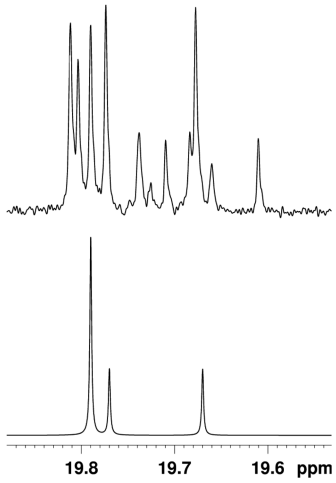

(b) actual (top) and predicted (bottom) ^{1}H NMR spectra

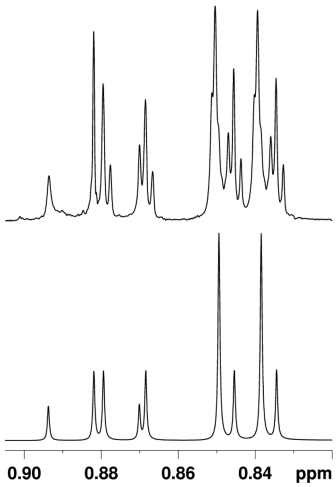

Figure 3. Comparison of the predicted and the experimental NMR spectra of the branched methyl group region for all-*syn*-**3c**.

terminal methyl group (C29 on the far right end). This triplet has the same predicted chemical shift in all of the isomers, so its value is not diagnostic. This leaves three major doublets in a ratio of 1:3:1 for the five branched Me groups of the major isomers. The smaller ones at 0.874 and 0.840 ppm are the left- and right-end methyl groups. As in the predicted ^{13}C NMR spectrum, the three middle methyl groups overlap, now at 0.844 ppm. The major resonances of the spectrum match the predictions of the all-*syn* isomer closely. Again, the match is clearly the best among all 16 predicted spectra.[10]

The experimental ^{1}H NMR spectrum again has a minor set of resonances; at least three minor doublets can be seen in the 1D spectrum. To find the other two minor resonances and to correlate all the resonances, we conducted a ^{1}H ^{13}C COSY experiment. Figure 4 shows two slices of the resulting spectrum: plot (a) is a higher slice that shows only the crosspeaks of the five major resonances, while plot (b) is a lower slice that shows both sets, but only the five minor crosspeaks are highlighted.

dx.doi.org/10.1021/jo4005298 | J. Org. Chem. 2013, 78, 4913−4918

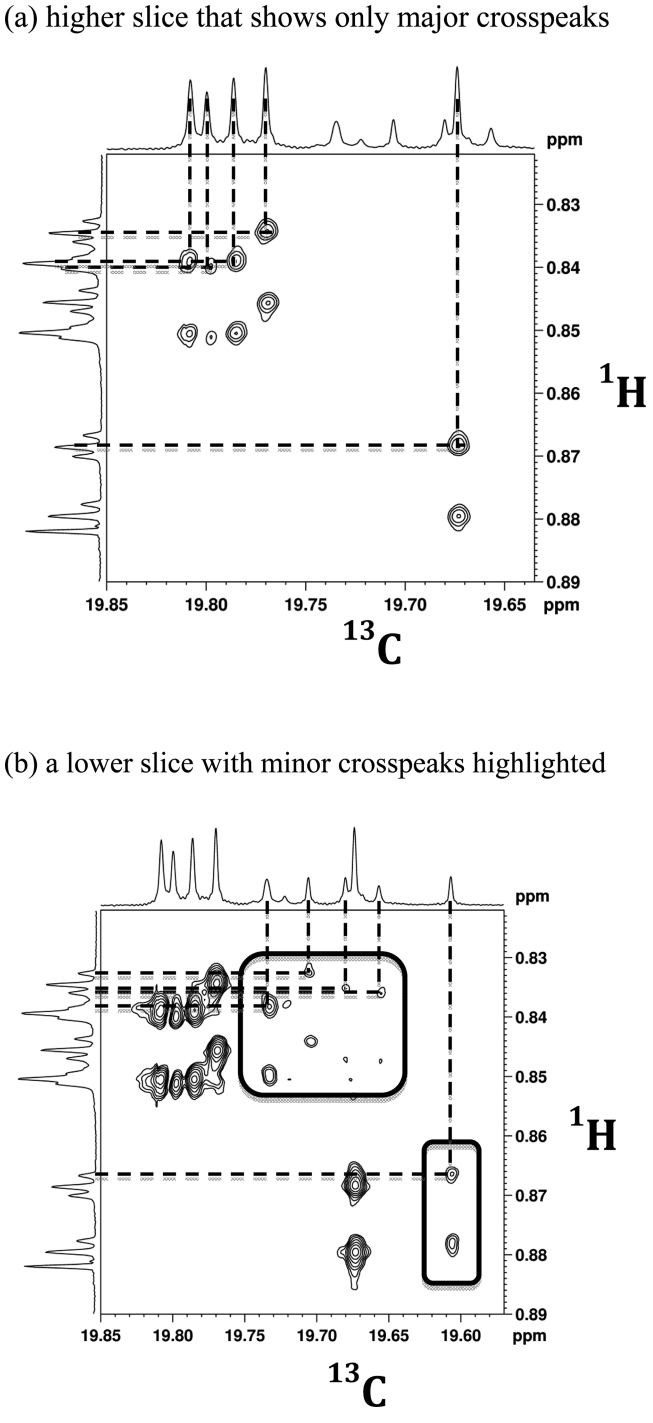

Figure 4. Branched methyl region of the ^{1}H ^{13}C COSY of all-*syn* **3c**.

All of the major peaks correlate as predicted by the model in Figure 2a, thus reinforcing the assignment of the major component of **3c** as all-*syn*. The reason that the largest doublet at 0.844 ppm in the ^{1}H NMR spectrum also appears to be further resolved into three peaks is revealed. The right shoulder comes from a minor isomer, correlated at 19.73 ppm in the ^{13}C spectrum, while the left shoulder comes from one of the middle carbons of the major isomer correlated at 19.81 ppm. The large center part correlates to the other two middle methyl groups in the major isomer at 19.80 and 19.79 ppm. So in the ^{1}H NMR spectrum, the prediction that three middle methyl groups of all-*syn*-**3c** would coincide is again wrong, but only just. This time, two resonances coincide, while the third is a smidge downfield (~1 ppb), appearing as a shoulder on the other two.

In contrast to the clear situation with the major set of five resonances, assignment of the minor set of five resonances is not straightforward. Four of the ^{13}C and ^{1}H resonances correspond well to other resonances predicted by the model (see unused resonances in Figure 2b): 19.73/0.842 ppm is a middle methyl group with a *syn*/*anti* (or *anti*/*syn* relationship) to its neighbors; 19.70/0.839 ppm is the right methyl group with an *anti* neighbor; 19.66/0.841 ppm is a middle methyl group with an *anti*/*anti* relationship; and 19.61/0.872 ppm is left methyl group with an *anti* neighbor.

There is also a minor peak at 19.68 ppm in the ^{13}C NMR that is not in the model set. This peak is only 10 ppb downfield from model peak 19.67, a left methyl group with a *syn* neighbor. However, if this assignment were correct, then that ^{13}C peak should correlate to a ^{1}H resonance at 0.874 ppm. Instead, it correlates to a resonance at 0.842 ppm.

In short, the major isomer in the new sample of **3c** is clearly the all-*syn* isomer. However, because of the simplicity of the model (it provides only seven resonances for all peaks in all possible isomers), we cannot yet assign the minor peaks. If they come from a single isomer, then one of the peaks (19.68 ppm) is poorly predicted in the ^{13}C NMR spectrum. If they come from a mixture of isomers, then there must be other minor peaks under the major peaks in varying ratios, so direct interpretation is not easy.

Analysis of the Spectra of 7. We next conducted a series of experiments trying to localize the stage of the synthesis where the minor isomer(s) originated. Small samples of key intermediates saved during the synthesis, especially the sample of **4** (Scheme 1), proved very helpful. This alkene could not be analyzed directly for stereochemical integrity because it already contains *E*/*Z* isomers from the Julia–Kocienski reaction. So about 2 mg of **4** was carefully hydrogenated (Pt, H_2, CH_2Cl_2/MeOH) to make a sample of **7** whose spectra were recorded as above.

The predicted spectrum of all-*syn*-**3b** was used for comparison, and the structures of **3b** and **7** are compared in Figure 5. Notice that while the right-end and middle fragments of **7** and all-*syn*-**3b** are the same, the left-end fragment is different. Sample **7** has two carbon atoms fewer than model **3b** at the left end, and its hydroxy group is protected with a

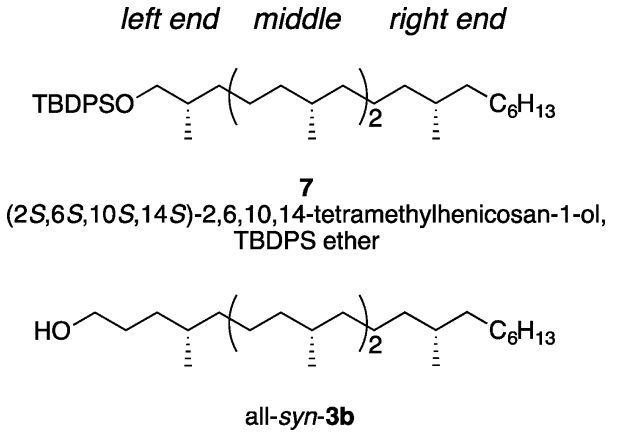

Figure 5. Predicted spectra of all-*syn*-**3b** are used to interpret the actual spectra of **7**. Only the middle and right-end predictions can be used because the left ends are different.

dx.doi.org/10.1021/jo4005298 | J. Org. Chem. 2013, 78, 4913–4918

TBDPS (*tert*-butyldiphenylsilyl) ether. Clearly the predicted left-end resonances for all-*syn*-**3b** cannot be applied to the left end of **7**.

The methyl region of the experimental ^{1}H NMR spectrum of **7** is shown in the top of Figure 6. There is only one set of resonances: four doublets and one triplet (the terminal methyl group on the end of the chain, C21). The resonances were assigned by 2D NMR experiments (see Supporting Information), and these assignments are collected in Table 1. Likewise, the ^{13}C NMR spectrum showed one set of resonances (bottom of Figure 6 and Table 1). Clearly this sample is a single isomer.

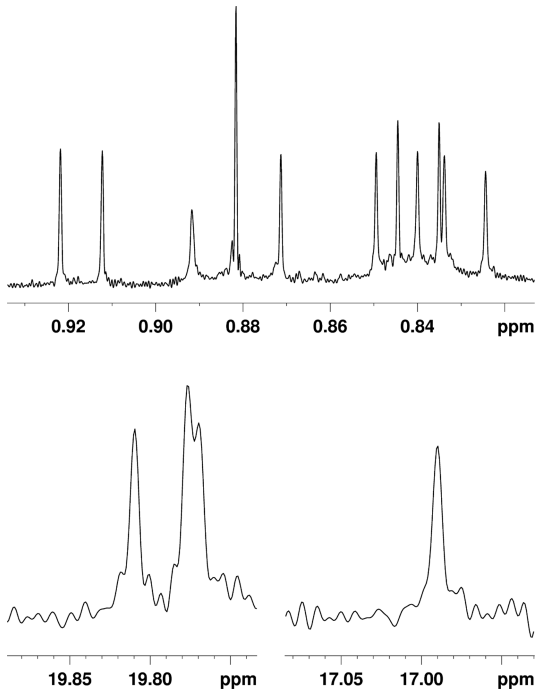

Figure 6. Expansions of the methyl regions of the ^{1}H (top) and ^{13}C (bottom) NMR spectra of **7**. The ^{1}H NMR expansion contains the terminal methyl group (C21) resonance, but the ^{13}C spectrum does not.

To assign the configuration of **7**, we compared the predicted methyl resonances of all-*syn* **7** with the actual resonances, as summarized in Table 1. The observed resonances for left-end methyl group (Me^{22}) appear at 0.917 ppm in the ^{1}H NMR spectrum and 16.99 ppm in the ^{13}C NMR spectrum. This pair of resonances has no equivalent in the model, but the values are not crucial to the stereochemical assignment because the chemical shifts of the next methyl group over (Me^{23}) also contain the information about whether the relationship of the two is *syn* or *anti*.

Table 1. Comparison of Methyl Resonances of the Actual Spectra of 7 with Predicted Resonances for the All-*syn* Isomer of 7 Derived from the Predicted Spectra of all-*syn*-3b; Data in ppm

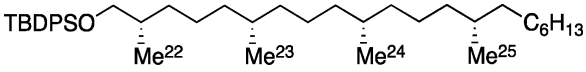

	^{1}H		^{13}C	
resonance	obsd	pred	obsd	pred
Me^{22}	0.917	*a*	16.99	*a*
Me^{23}	0.830	0.844[b]	19.76	19.79[b]
Me^{24}	0.845	0.844[b]	19.80	19.79[b]
Me^{25}	0.840	0.840[c]	19.76	19.77[c]

[a]The model does not predict the left-end resonance. [b]Middle resonance, see Figure 2. [c]Right-end resonance, see Figure 2.

Now compare the predicted and actual resonances for the remaining Me groups (Me^{23}, Me^{24}, and Me^{25}) in structure **7**, starting at the right end of the molecule. In both the ^{1}H and the ^{13}C NMR spectra, the actual and predicted resonances for the right-end methyl group (Me^{25}) and its neighbor (Me^{24}) are spot on or almost spot on. At 0.830 ppm (^{1}H) and 19.76 (^{13}C) ppm, the actual resonances of the next methyl group in (Me^{23}) are slightly different from both Me^{24} and the prediction. As above, this is again a deficiency of the model, which provides only a single middle resonance that is used to model both Me^{23} and Me^{24}. It is sensible that the model is spot on for Me^{24}, which is further away from the left end (the part that differs between the model and the actual sample), and slightly off for Me^{23}, which is closer to the left end.

The values of the experimental ^{1}H NMR spectra of **7** in Table 1 are much closer to the predicted values for the all-*syn* isomer of **3b** than to any of the other seven isomers.[10] Thus, both the relative configuration of the sample (all-*syn*) and the high level of purity (≥95%) are confirmed.

These experiments show that the four stereocenters of key synthetic intermediate **4** are intact and have the configurations predicted by the various asymmetric reactions used to introduce them (Scheme 1). Thus, the minor stereoisomer(s) in sample **3c** must have formed in a late stage of the synthesis, during or after the coupling of the last two fragments **4** and **5** (Scheme 1). Primary candidate steps for the epimerization are the Julia–Kocienski reaction (the aldehyde reactant has an adjacent stereocenter) and the final hydrogenation reaction (alkene migration to form a trisubstituted double bond, prior to hydrogenation, results in loss of stereointegrity[14]).

Finally, this exercise establishes a new left-end model compound with a CH_2OTBDPS group from which spectra of saturated isoprenoids and related reduced polyketides can be predicted. Compounds such as **7** terminating in CH_2OTBDPS on the left end will have a chemical shift of 0.830 and 19.76 ppm for the left-end methyl group (Me^{22}) if it is *syn* to the next methyl group (Me^{23}). On the basis of the established trends with **3a**, we predict that Me^{22} will resonance a little further upfield in both the ^{1}H and ^{13}C NMR spectra if it is *anti* to Me^{23} (about 2 and 60 ppb, respectively, see Figure 2). From the chemical shifts in Table 1, small upfield adjustments also need to be made for the resonances of Me^{23} in the *syn*/*syn* isomer to predict the spectra of isomers with this group *syn*/*anti* (or *anti*/*syn*) and *anti*/*anti* to Me^{22}/Me^{24}. The magnitudes of the adjustments can again be estimated from the values for the analogous middle methyl groups in Figure 2.

These new resonances can be added to the existing middle (used for Me^{24}) and right (used for Me^{25}) resonances in Figure 2 to fill out predicted spectra for any isomer of **7** or a higher oligomer. Because the model **7** has four resonances, every isomer of **7** (or a higher oligomer) will also have four predicted resonances. This is an improvement over the use of **3a** to model **3b** and **3c**, where two or three middle Me groups have the same predicted chemical shift in some isomers, even though in reality there are small differences.

dx.doi.org/10.1021/jo4005298 | J. Org. Chem. 2013, 78, 4913–4918

CONCLUSIONS

In summary, for the first time it has been possible through NMR spectroscopy both to assess isomer purity and to assign relative configurations of saturated oligoisoprenoids such as **3c**. Recent predictions of the methyl regions of the ^{1}H and ^{13}C NMR spectra of all 16 stereoisomers of **3c** enabled this analysis.[10] The predicted ^{1}H NMR spectrum of all-*syn*-**3c** is very close to the actual spectrum, but the predicted ^{13}C NMR spectrum proved to be too simple in one aspect: the three resonances from the middle methyl groups were predicted to coincide because they all have the *syn*/*syn* relationship, but they did not. However, the observed differences between predicted and actual spectra were small compared to the differences expected for other stereoisomers, so the value of the ^{13}C NMR predictions was not compromised.

The analysis of the synthetic sample of **3c** showed that the all-(*S*) (all-*syn*) isomer was indeed the major component, present to the extent of about 70%. Unexpectedly, a minor stereoisomer component (or components) was present to the extent of about 30%. We cannot yet identify the minor component or pinpoint where it was introduced. However, by similar comparison of actual and predicted spectra, we could show that **7** (derived from a key synthetic intermediate **4** bearing four of the five stereocenters) is both pure (>90%) and has the expected all-(*S*) configuration. This narrows the source of the problem to the last few steps of the synthesis.

Perhaps most importantly, the values from the predicted spectra of compounds like **3c** can now be leveraged to related compounds bearing different right or left ends. As an example, intermediate **7** with four stereocenters has a left end different from that of **3a**−**c**. Even though we only made one of the eight possible stereoisomers of **7**, we can now combine the new data obtained for **7** with the data for **3a** to assemble predicted spectra of the other seven isomers of **7** and its higher oligomers. This ability to directly analyze complex, saturated oligoisoprenoids is a powerful tool to clarify a heretofore cloudy situation with respect to stereoisomer structure and purity of synthetic and natural samples.

EXPERIMENTAL SECTION

The synthesis of intermediates **3c** and **6** followed published routes. Experimental details and characterization data can be found in refs 4 and 11. Detail reaction conditions and yields are shown in the Supporting Information, Schemes S1 and S2.

***tert*-Butyldiphenyl(((2*S*,6*S*,10*S*,14*S*)-2,6,10,14-tetramethylhenicosyl)oxy)silane (7).** Dry 10 wt % Pt/C (0.003 g, 0.002 mmol) was added to **6** (0.003 g, 0.005 mmol) in MeOH/CH_2Cl_2 (3:1, 1 mL). The suspension was flushed three times with H_2 (three vacuum/H_2 cycles) and stirred under an atmosphere of H_2 (1 atm, balloon) at rt for 24 h. The reaction mixture was filtered through a silica gel plug and concentrated to yield the hydrogenation product **7** quantitatively. ^{1}H NMR ($CDCl_3$, 700 MHz, ppm) δ 7.66 (d, J = 6.8 Hz, 4 H), 7.41 (t, J = 7.3 Hz, 2 H), 7.37 (t, J = 7.2 Hz, 4 H), 3.51 (dd, J = 5.6, 9.8 Hz, 1 H), 3.43 (dd, J = 6.4, 9.8 Hz, 1 H), 2.22 (t, J = 7.6 Hz, 1 H), 1.63 (m, 3 H), 1.13−1.42 (m, 30 H), 1.05 (s, 9 H), 0.92 (d, J = 6.7 Hz, 3 H), 0.88 (t, J = 7.0 Hz, 3 H), 0.82−0.85 (m, 9 H); ^{13}C NMR ($CDCl_3$, 175 MHz, ppm) δ 135.61, 134.13, 134.11, 129.43, 127.52, 68.88, 37.42, 37.40, 37.38, 37.34, 37.05, 35.71, 33.46, 32.80, 32.76, 32.75, 31.92, 29.99, 29.69, 29.66, 29.65, 29.64, 29.60, 29.40, 29.36, 27.08, 26.85, 24.47, 24.45, 24.38, 22.69, 19.79, 19.75, 19.74, 19.30, 16.97, 14.13.

ASSOCIATED CONTENT

Supporting Information

Copies of NMR spectra of **3c**, **4**, and **7**. This material is available free of charge via the Internet at http://pubs.acs.org.

AUTHOR INFORMATION

Corresponding Author

*E-mail: a.j.minnaard@rug.nl; curran@pitt.edu.

Notes

The authors declare no competing financial interest.

ACKNOWLEDGMENTS

The Groningen group thanks NWO-CW for a VICI grant to A.J.M. The Pittsburgh group thanks the National Institutes of Health for funding this work and for funds to help purchase a 700 MHz NMR spectrometer.

REFERENCES

(1) Moody, D. B.; Ulrichs, T.; Mühlecker, W.; Young, D. C.; Gurcha, S. S.; Grant, E.; Rosat, J.-P.; Brenner, M. B.; Costello, C. E.; Besra, G. S.; Porcelli, S. A. *Nature* **2000**, *404*, 884−888.

(2) Zetta, L.; Gatti, G.; Audisio, G. *Macromolecules* **1978**, *11*, 763−766.

(3) Crich, D.; Dudkin, V. *J. Am. Chem. Soc.* **2002**, *124*, 2263−2266.

(4) (a) van Summeren, R. P.; Moody, D. B.; Feringa, B. L.; Minnaard, A. J. *J. Am. Chem. Soc.* **2006**, *128*, 4546−4547. (b) Ferrer, C.; Fodran, P.; Barroso, S.; Gibson, R.; Hopmans, E. C.; Sinninghe Damsté, J.; Schouten, S.; Minnaard, A. J. *Org. Biomol. Chem.* **2013**, *15*, 2482−2492.

(5) de Jong, A.; Arce, E. C.; Cheng, T.-Y.; van Summeren, R. P.; Feringa, B. L.; Dudkin, V.; Crich, D.; Matsunaga, I.; Minnaard, A. J.; Moody, D. B. *Chem. Biol.* **2007**, *14*, 1232−1242.

(6) Matsunaga, I.; Bhatt, A.; Young, D. C.; Cheng, T.-Y.; Eyles, S. J.; Besra, G. S.; Briken, V.; Porcelli, S. A.; Costello, C. E.; Jacobs, W. R.; Moody, D. B. *J. Exp. Med.* **2004**, *200*, 1559−1569.

(7) Scharf, L.; Li, N.-S.; Hawk, A. J.; Garzón, D.; Zhang, T.; Fox, L. M.; Kazen, A. R.; Shah, S.; Haddadian, E. J.; Gumperz, J. E.; Saghatelian, A.; Faraldo-Gómez, J. D.; Meredith, S. C.; Piccirilli, J. A.; Adams, E. J. *Immunity* **2010**, *33*, 853−862.

(8) Kwan, D. H.; Sun, Y.; Schulz, F.; Hong, H.; Popovic, B.; Sim-Stark, J. C. C.; Haydock, S. F.; Leadlay, P. F. *Chem. Biol.* **2008**, *15*, 1231−1240.

(9) Ohrui, H. *Proc. Jpn. Acad., Ser. B* **2007**, *83*, 127−135.

(10) Yeh, E. A.; Kumli, E.; Damodaran, K.; Curran, D. P. *J. Am. Chem. Soc.* **2013**, *135*, 1577−1584.

(11) (a) van Summeren, R. P.; Reijmer, S. J. W.; Feringa, B. L.; Minnaard, A. J. *Chem. Commun.* **2005**, 1387−1389. (b) Naito, J.; Kuwahara, S.; Watanabe, M.; Decatur, J.; Bos, P. H.; Van Summeren, R. P.; Horst, B. T.; Feringa, B. L.; Minnaard, A. J.; Harada, N. *Chirality* **2008**, *20*, 1053−1065.

(12) Blakemore, P. R. *J. Chem. Soc., Perkin Trans. 1* **2002**, 2563−2585.

(13) Traficante, D. D.; Nemeth, G. A. *J. Magn. Reson.* **1987**, *71*, 237−245.

(14) (a) Dandapani, S.; Jeske, M.; Curran, D. P. *J. Org. Chem.* **2005**, *70*, 9447−9462. (b) Teichert, J. F.; den Hartog, T.; Hanstein, M.; Smit, C.; ter Horst, B.; Hernandez-Olmos, V.; Feringa, B. L.; Minnaard, A. J. *ACS Catal.* **2011**, *1*, 309−315.